Electronic structure of point defects in rutile TiO_2

Naichang Yu and J. Woods Halley
School of Physics and Astronomy, University of Minnesota, Minneapolis, Minnesota 55455
(Received 25 July 1994; revised manuscript received 22 September 1994)

We present results of a computation of the electronic structure of point defects in reduced rutile using a semiempirical self-consistent method. Calculations on models of both titanium interstitials and oxygen vacancies are reported. We find donor levels in the range 0.7–0.8 eV for isolated defects in each case. The defects have an effective screening radius of less than 5 Å. We also report results on clusters of defects. These suggest that a model in which the screening charges of multiple defects are added would be quite accurate for systems with multiple defects. Comparison of our results with infrared experiments suggests the presence of defect clustering in nearly stoichiometric rutile, as proposed earlier on the basis of other experiments.

I. INTRODUCTION

Titanium dioxide is a technologically important material, and is one of the most studied transition-metal oxides both experimentally and theoretically.[1] The band structure of the perfect crystal has been calculated by various empirical and first-principles methods, both with density-functional with local-density approximations and with Hartree-Fock approximations.[2–4] Recent calculations predict a geometric structure that agrees well with experimental results, though the predicted optical band gaps disagree with experimentally observed ones, as they do for most transition-metal oxides. Naturally occurring rutile, however, is almost always reduced, and many important properties and functions of the oxide depend on the defect structure. For example, catalytic behavior and the growth and dissolution rates of the oxide in electrochemical cells depend critically on the electronic density of states in the bulk band gap.[5] It is generally agreed that rutile is an *n*-type material that is oxygen deficient or metal rich, but whether titanium interstitials or oxygen vacancies are the dominant defects has not been definitively established. Experimental exploration of electronic states associated with defects arising as a result of oxygen deficiency revealed infrared absorption arising from an impurity band about 0.7 eV below the conduction-band edge. Estimates indicated that oxygen vacancies could be responsible for these states.[6] Experiments on the dependence of the electrical conductivity and various diffusion rates on the oxygen partial pressure[7] do not clearly establish whether titanium interstitials or oxygen vacancies are the dominant defect. The most recent such experiments[8] were interpreted as evidence of titanium interstitials.

The electronic structure of rutile containing these defects, however, has received little theoretical attention, partly because of the computational difficulties arising from the disorder and partly because of the general problems associated with computing the electronic structure of transition-metal oxides. An early one-electron tight-binding model[9] for the oxygen vacancy assumed a hard-sphere model for the potential associated with an oxygen vacancy. In earlier papers, we applied the equation of motion method to study the electronic structure of disordered rutile,[10–12] using a phenomenological Yukawa potential to describe the oxygen vacancies. Such a scheme allows one to study large samples of the material, with multiple oxygen vacancies. However, because of the strong interaction of electrons on transition-metal ions, a self-consistent calculation that incorporates the interaction effect is desirable. Recently, a first-principles calculation based on the local-density approximation has been reported for a single oxygen vacancy on a surface.[13] A single donor level 0.3 eV below the conduction-band edge was found. In this paper, we present a self-consistent calculation of the electronic structure of both titanium interstitials and oxygen vacancies in rutile TiO_2 using a semiempirical method which we have recently also applied to rutile surfaces.[14]

II. METHOD

Details of our semiempirical method for the application of self-consistent methods to tight-binding studies of the electronic structure of transition metal-oxides appear in Ref. 14. We provide a brief description of the method in the Appendix. In fact, the computational essence of our approach can be stated quite simply. The advantage of the more formal derivation of the method in the Appendix is that it clarifies how our approximations may be improved.

The effective one-electron Schrödinger equation which we solve is

$$\left[\frac{\partial E_k}{\partial Q_k}+\sum_{j\neq k}\frac{e^2Q_j}{R_{kj}}\right]\langle k\mu|\lambda\rangle+\sum_{i\neq k,\nu}\left[t_{k,\mu;i,\nu}+v^{(1)}_{k,\mu;i,\nu}+(1-\delta_{i,k})\frac{e^2}{R_{ki}}\delta_{\sigma_\nu,\sigma_\mu}Q_{k,\mu;i,\nu}\right]\langle i,\nu|\lambda\rangle\,,$$
$$=\epsilon_\lambda\langle k,\mu|\lambda\rangle-\mu_c\langle k,\mu|\lambda\rangle\,, \quad (1)$$

where the one-electron pseudowavefunctions ψ_λ are expressed in terms of a tight-binding basis of orbitals labeled i,μ (i is a site label) by the coefficients $\langle i,\mu|\lambda\rangle$. μ_c is the chemical potential (or Fermi energy). Q_i is the charge associated with site i and calculated from $\langle i,\mu|\lambda\rangle$. The term involving $Q_{k,\mu;i,\nu}$ describes exchange interactions. It is dropped in the calculations presented here. To obtain an expression for the intrasite term $\partial E_k/\partial Q_k$, we use the experimentally determined ionization potentials of the relevant ions. When the ion has integer numbers of electrons, E_l is taken to be a constant minus the sum of the relevant ionization potentials. For noninteger numbers Q_l of electrons, we use a spline fit or a linear interpolation between the integer values. The results for $\partial E_l/\partial Q_l$ for the ions of interest in rutile are given in Ref. 14. $\partial E_l/\partial Q_l$ is nearly linear in Q_l. In a Hubbard model, $\partial E_l/\partial Q_l$ would be precisely linear, and the slope would be the Hubbard U. Interpreted in this way, one finds effective U's in the range 10–20 eV for rutile. In our calculations we use the functions determined from ionization potentials, except that a constant is added empirically as discussed in Sec. III. [The empirical constant may be regarded in part as compensating for the errors in approximation (A16).]

In general, the calculational procedure using this approach is to choose a set of initial values of Q_l (and $Q_{l,\kappa;j,\nu}$ if they are used), and solve the one-electron problem represented by (1). Using the eigenfunctions, Q_l (and $Q_{l,\kappa;j,\nu}$) are then recalculated using (A10) and (A13), and the procedure is iterated to self-consistency.

In the calculations reported here, we neglect the terms of form $v^{(1)}_{k,\mu;i,\nu}$ and use an empirical estimation of the hopping integrals $t_{l,\kappa;j,\nu}$ as described in Sec. IV.

III. MODEL FOR RUTILE

We use a tight-binding model for rutile which contains five d states per titanium site, and three p states and one s state per oxygen site. We reference the orbitals to a Cartesian coordinate system as illustrated in Fig. 1. We adopt the same hopping integrals as in the fully phenomenological model of Vos,[3] summarized in our earlier work.[11] The diagonal energies of the orbitals are calculated self-consistently as described in Sec. II, using Ewald techniques[15] to obtain the Coulomb energy in Eq. (1). With this parametrization, as discussed in Ref. 14, we find that the calculated optical gap is not in agreement with the experimental one. We compensate for this discrepancy, which may result from violations of Koopmans' theorem[16] or from errors in approximation (A15) by adding an empirically determined constant to the diagonal parameters of the model.[14] In particular, the diagonal energies of the titanium atoms are adjusted by -0.45 eV, and those of the oxygen orbitals are adjusted up by 4.2 eV. We make this adjustment consistently in all subsequent calculations for samples with impurities. The self-consistent calculations are done with a supercell of $3\times3\times5$ unit cells. ($\sim$15 Å on each side, containing 270 atoms). Periodic boundary conditions are applied in all three dimensions.

For the uniform system, this empirical model predicts a system slightly more covalent than predicted by a self-consistent Hartree-Fock calculation.[17] (The Hartree-Fock calculation predicts an optical gap of 10 eV compared to the experimental one of 3 eV.) At self-consistency, the (electronic plus nuclear) charge on the titanium atom is $+2.18|e|$, and that on the oxygen atom is $-1.09|e|$. Some other details of the comparison of the electronic structure predicted by our model for stoichiometric rutile without surfaces appear in Ref. 14, where they are compared with other calculations and with experiment.

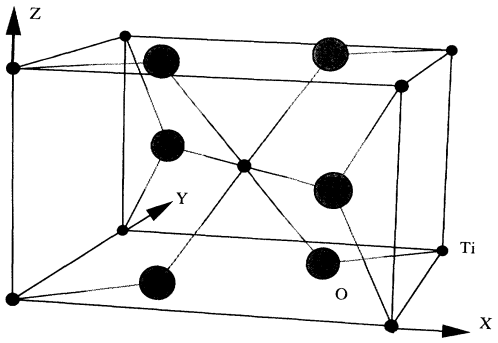

FIG. 1. A unit cell of rutile TiO_2. The smaller darker circles represent the titanium atoms; the larger lighter circles represent oxygen atoms.

IV. TITANIUM INTERSTITIALS

We first describe the study of titanium interstitials. In the rutile structure the oxygen atoms bonded with a titanium atom form an approximate octahedron. However, only half of the available octahedral sites are occupied. The two unoccupied octahedral sites per rutile unit cell at the center of the four (100) and (010) surfaces of the rutile unit cell. These unoccupied sites are apparently favorite sites for the titanium interstitials. The octahedrons around these interstitial titanium atoms are more distorted than the octahedrons occupied by normal lattice titanium atoms, and we modify the hopping integrals by linearly extrapolating the phenomenological hopping integrals given by Vos,[3] except that, for the closest Ti-O pair in the interstitial-oxygen octahedron, we use the same hopping integral as for the normal titanium atoms. (This exception is made because we expect that atomic relaxation of the oxygen atoms around the titanium interstitial will make the octahedron like the octahedron around a normal lattice titanium atom. A full treatment of atomic relaxation around the defects has not been made in the context of this model and is reserved for future work.) Table I summarizes the geometry and hopping integrals we use, including those between the interstitials and their neighbors.

We study a cluster of $(3\times4\times4)$ rutile unit cells, of 289 atoms, with one titanium interstitial, located in the cell at the middle of the cluster. Periodic boundary conditions are applied in all three dimensions. A self-consistent solution of this system indicates that the conduction-

TABLE I. Hopping integrals between neighboring atoms.

		a (Å)	E (eV)	a (Å)	E (eV)	a (Å)	E (eV)	a (Å)	E (eV)
Ti-O	$pd\sigma$	1.64	−2.30	1.94	−2.30	1.99	−2.30	2.23	−1.15
Ti-O	$pd\pi$	1.64	1.15	1.94	1.15	1.99	1.15	2.23	0.575
Ti-O	$pd\delta$	1.64	−2.5	1.94	−2.50	1.99	−2.50	2.23	−1.25
O-O	$pp\sigma$	2.52	0.600	2.78	0.400	2.96	0.250		
O-O	$pp\pi$	2.52	−0.120	2.78	−0.080	2.96	−0.05		
Ti-Ti	$dd\sigma$	2.30	−1.0	2.73	−0.75	2.96	−0.500	3.57	−0.200
Ti-Ti	$dd\pi$	2.30	0.52	2.73	0.39	2.96	0.26	3.57	0.104
Ti-Ti	$dd\delta$	2.30	−0.07	2.73	−0.05	2.96	−0.035	3.57	−0.014

band edge of the host lattice is little altered by the introduction of the interstitial. However, two impurity states appear below the conduction-band edge, at 0.19 and 0.80 eV below the conduction-band edge. Figure 2(a) shows the density of states projected on the titanium interstitial and its six octahedral neighbors, obtained by broadening the levels with a Lorentzian of width 0.1 eV. The local densities of states reveal that the wave function of the impurity state 0.8 eV below the conduction-band edge has little amplitude on the six nearest-neighbor oxygen atoms around the titanium interstitial. Transitions from this occupied state to the bottom of the conduction band would account well for the position of the experimentally observed peak in infrared absorption. Figure 2(a) shows the self-consistent charge distribution on the interstitial and its six nearest-neighbor oxygen atoms. The titanium interstitial has 0.60 more electrons on it than other titanium atoms in the crystal. Extra electrons are deposited on the six oxygen atoms forming the octahedron surrounding the titanium interstitial. Each of the two oxygen atoms closest to the interstitial (1.64 Å away from the interstitial) has charge $-1.38|e|$ (corresponding to a screening charge of $=-0.29|e|$), while the other four have charge $-1.25|e|$ (screening charge $-0.16|e|$.) The atoms farther away have much smaller screening charges, the maximum being $0.04|e|$. It is also interesting to look at the self-consistent diagonal energies associated with orbitals on these atoms. The $3d$ orbitals on the titanium interstitial have a diagonal energy of -5.83 eV, compared with -6.4 eV far away from the interstitial. The diagonal oxygen $2p$ orbital energies on the nearest neighbors of the interstitial are -13.7 eV on the atom 1.64 Å away from the interstitial and -11.7 eV on the atoms 2.27 Å away from the interstitial, compared with -10.5 eV far away from the interstitial. These results are also summarized in Fig. 2(a).

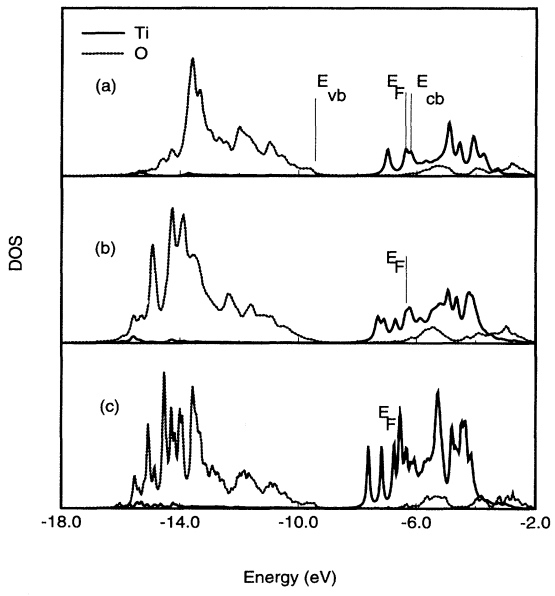

FIG. 2. The local density of states on the titanium interstitials and their oxygen neighbors for the three configurations given in Fig. 3.

Considering the semiempirical nature of our calculation, it is interesting to see the stability of our result with respect to the empirical parameters. We have varied hopping integrals between the interstitial and its neighboring oxygen atoms by 20%, and also changed the position of the titanium interstitial atom by about 0.15 Å, and found that the impurity level is remarkably stable with respect to these changes. The energy of the impurity level changes less than 0.05 eV for the cases we explored.

We find that strong interference between interstitials occurs only if the octahedra surrounding two interstitials share common oxygen atoms. This can happen only in two cases: when the two interstitials are on neighboring faces of the rutile unit cell, or when the two interstitials are on equivalent sites on two neighboring unit cells in the [001] direction. We first report results on the latter case as shown in Fig. 3(b). The interstitials are only about 3 Å apart. The Fermi energy in this case touches the bulk conduction-band edge. There are levels at 0.35, 0.74, and 0.95 eV below the conduction band edge. Figure 2(b) shows the local density of states on the titanium interstitials and the nearest-neighbor oxygen atoms, obtained by a Lorentzian broadening of width 0.1 eV. Again the states in the band gap have mainly titanium $3d$ character. The charges on the interstitials are slightly different from the single-interstitial case. Each interstitial has charge $1.49\ |e|$. The two oxygen atoms closest (1.64 Å) to each interstitial have charges $-1.39\ |e|$ each, similar to the single-interstitial case. The two oxygen atoms shared by the interstitial octahedrons have charge $-1.35|e|$. Unlike the single-interstitial case, appreciable changes also take place on the nearest-neighbor titanium atoms to the interstitial. These atoms show screening charges of about $-0.1|e|$. The charges

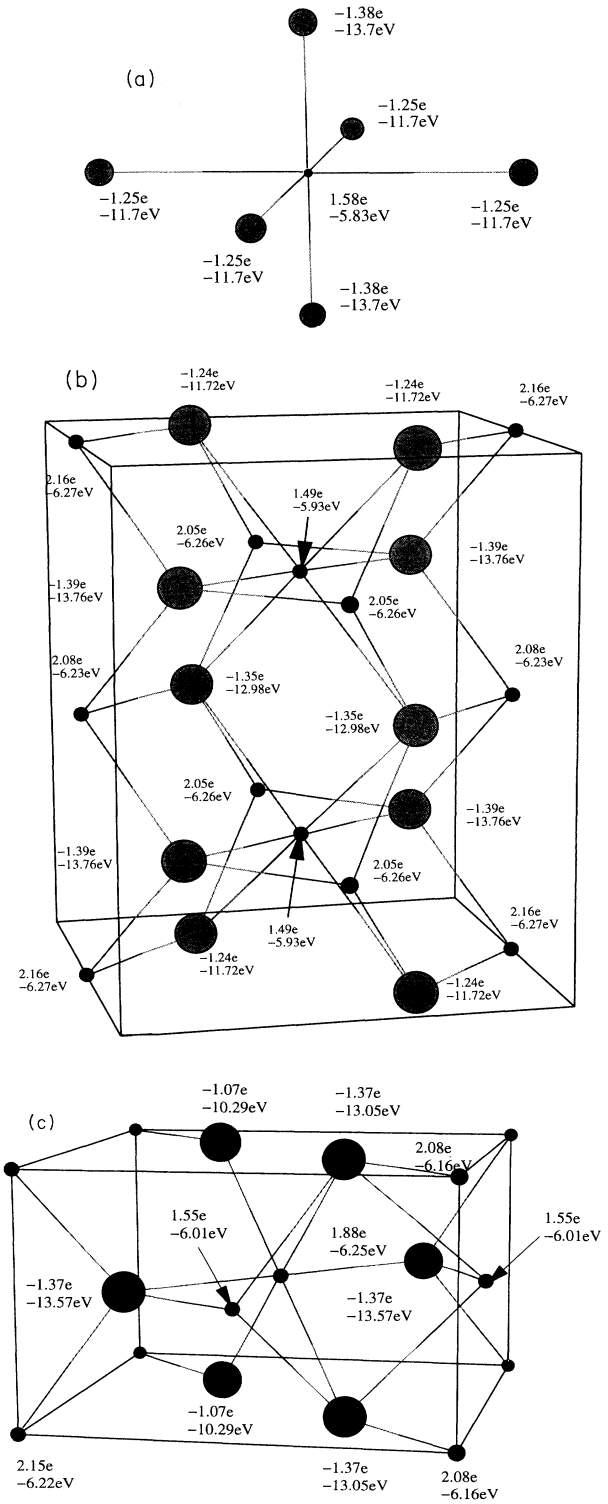

FIG. 3. Three configurations of titanium interstitials and the self-consistent charge and orbital energies on the atoms near the interstitials. On titanium atoms we give the ϵ_{3d}, on oxygen atoms we give ϵ_{2p}. (a) shows the titanium interstitial and the six oxygen atoms around the interstitial. (b) shows two interstitials at two neighboring rutile unit cells in the [001] direction. The interstitials are marked by arrows. (c) shows two interstitials in the same rutile unit cell.

and orbital energies for this case are summarized in Fig. 3(b).

The second possible configuration in which two interstitial octahedron share common oxygen atoms is that in which the two interstitials are on neighboring faces of a rutile unit cell. This is the configuration that Aono and Hasiguti[18] recently used as a model to explain the electron paramagnetic resonance (EPR) spectra they obtained on slightly reduced rutile. Figure 2(c) shows the self-consistent local density of states which we calculated in this case on the interstitials and their nearest-neighbor oxygen atoms. The density of states is similar to that found in the previous case. The impurity levels in this case extend to 1 eV below the conduction-band edge. The charges and orbital energies on atoms surrounding the interstitials are shown in Fig. 3(c). The charge on the interstitials is $1.55|e|$, the same as the single-interstitial case. The two closer oxygen neighbors for each interstitial again have charges $-1.37|e|$, very similar to the single-interstitial case and the double-interstitial case presented above. The two common oxygen neighbors of the two interstitial have charges of $-1.37|e|$ each (screening charge $-0.27|e|$), close to the previous double-interstitial case. The screening charge on these oxygen neighbors is close to that which would be obtained by simply summing the screening charge ($-0.15|e|$) arising from each interstitial alone. The exception to the simple addivity of the screening charges is the screening charge on the titanium at the center of the cell shown in Fig. 3(c). Because of the complex bonding of that titanium atom to the nearest-neighbor oxygen atoms of the interstitials, the screening charge on the atom is $-0.3|e|$, far above the result of simple addition of screening charges caused by individual interstitials.

The good local screening of the impurity charge suggests that the interference between interstitials far apart is small. We studied clusters with various numbers of impurities, and found that as long as the interstitials are far apart so that they do not share oxygen atoms as nearest neighbors, the electronic structure is close to a simple superposition of that of individual interstitials. For example, putting four interstitials on a square 5 Å on each side produced three levels at -6.99 eV and one at -7.01 eV, compared with one level at -6.98 eV for the single-interstitial case. Examination of the charges also confirms there is little interference between the interstitials.

V. OXYGEN VACANCIES

We model an oxygen vacancy as an oxygen site characterized by an s orbital with the same hopping integrals between the orbitals on the vacancy and on other sites as the s orbital had when the site was occupied by oxygen. The diagonal energy of the orbital associated with the vacancy site is self-consistently determined through the Coulomb potential at the site plus an empirically determined constant. The constant is taken to be 9.0 eV. This value was selected so that self-consistent calculations yield a donor energy level 0.7 eV below the conduction-band edge, consistent with the position of the observed

infrared absorption. Figure 4(a) shows the local density of states on the vacancy, its nearest-neighbor titanium atoms, and some of their oxygen neighbors. It is seen that the impurity state 0.7 eV below the conduction-band edge consists mainly of a titanium $3d$ component, and some component on the vacancy.

Each oxygen atom in the host rutile lattice is covalently bonded with three nearest-neighbor titanium atoms, as shown in Fig. 5(a). The oxygen atom and the three titanium atoms are coplanar. In this model, an oxygen vacancy severely affects the electronic structure around the vacancy and the three titanium atoms. Figure 5(a) also shows the self-consistent potential and charge distribution on the oxygen vacancy and its three nearest-neighbor titanium atoms. It is found that, due to the accumulation of charges on the titanium atoms around the vacancy, the self-consistent diagonal energies are increased relative to the uniform system. On the two equivalent titanium atoms, $\epsilon_{3d} = -6.22$ eV, compared with the potential for the uniform system $\epsilon_{3d} = -6.40$ eV. On the other hand, the third titanium atom is not the favorite atom for deposition of a screening electron due to the dangling-bond effect: its on-site energy is lowered to -6.50 eV.

The screening charge on the vacancy is almost restricted to the vacancy and its nearest-neighbor titanium atoms. The charge on the vacancy is $-0.46|e|$; the charges on the nearest-neighbor titanium atoms are nearly the same, the charges on the two equivalent titanium atoms being $2.01|e|$ (screening charge $-0.17|e|$) and on the third titanium atom being $2.04|e|$ (screening charge $-0.14|e|$). The charge of the vacancy is thus nearly compensated for in the first shell: only $0.15|e|$ is spread over all the other atoms.

We find that strong interaction between the oxygen vacancies occurs only if the two vacancies share a titanium atom as common nearest neighbor. As examples, we studied two such pairs of vacancies, one in which the two vacancies occupy opposite vertices of the octahedron surrounding a titanium atom, and another in which the two vacancies share an edge of an octahedron. Figure 5(b) shows the two oxygen vacancies occupying opposite vertices of an octahedron and their titanium nearest neighbors. Such a pair of vacancies produced two energy levels in the bulk band gap, one at 0.22 eV below the conduction-band edge, and the other one at 1.28 eV below the conduction-band edge as shown in the density of states in Fig. 4(b). The charge distribution is again rather local. Figure 5(b) shows the self-consistent potential and charge on the titanium atoms closest to the oxygen vacancies. The oxygen vacancies and the five nearest-neighbor titanium atoms hold $-1.93|e|$ screening charges. Only $-0.25|e|$ screening charges are spread outside the nearest neighbor. Furthermore, the screening charge distribution for the two vacancies is close to that obtained by simply adding the screening charges arising from two separate vacancies.

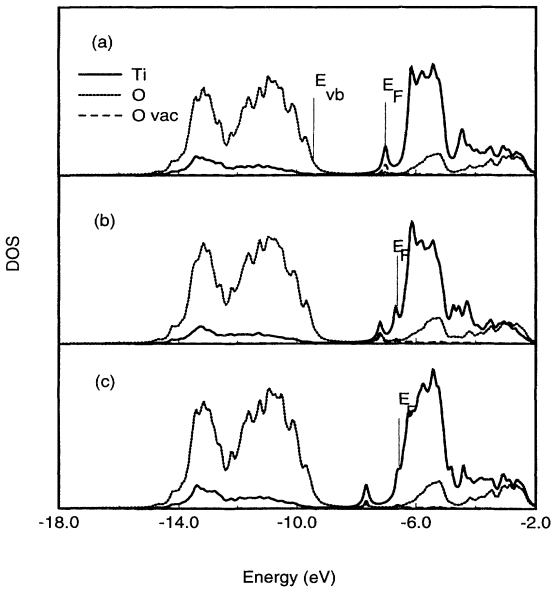

FIG. 4. Local density of states for the three configurations of vacancies given in Fig. 5.

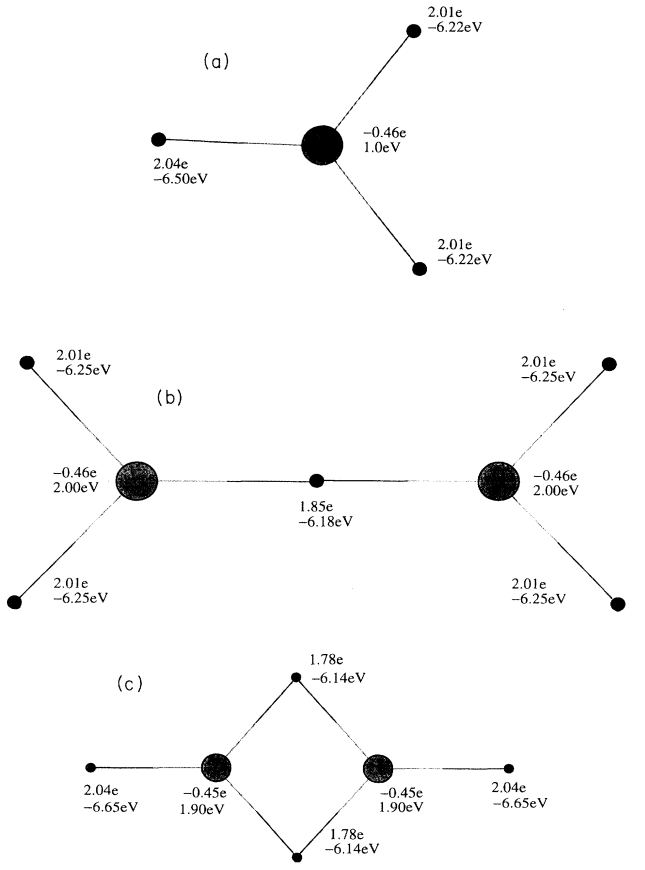

FIG. 5. Three configurations of oxygen vacancies and their nearest-neighbor titanium atoms. Also shown are the self-consistent charges on the atoms and the (ϵ_{3d} orbital on the titanium atoms or orbital at the vacancy) energies. Vacancies are represented by lighter circles. Titanium atoms are represented by darker, smaller circles. (a) One oxygen vacancy. (b) Two vacancies in a line with a titanium atom. (c) Two vacancies that are also near neighbors in the host rutile structure.

Another pair of vacancies is shown in Fig. 5(c), where the two vacancies share an edge of the octahedron around one titanium atom. Also shown in Fig. 5(c) are the self-consistent charge distribution and the diagonal matrix elements associated with orbitals on the atoms surrounding the vacancies. Similar to the previous case, the two oxygen vacancies and their nearest-neighbor titanium atoms hold $-1.98|e|$ screening charge, and only 0.20 electron is spread outside the nearest neighbor. The charge distribution around the vacancy again is close to that obtained by simple addition of the screening charge distribution arising from single vacancies. This pair of vacancies produces a pair of energy levels in the band gap of the bulk rutile, one at 0.26 eV and the other 1.15 eV below the band edge. Both these two levels are occupied. Figure 4(c) shows the local density of electronic states around the vacancies. Again the states in the bulk band gap have a small oxygen component.

The above analysis indicates that the charge redistribution is restricted to the nearest neighbors of the oxygen vacancies, and suggests that oxygen vacancies which do not share a titanium neighbor will behave essentially independently with regard to their electronic structure. We find this to be approximately correct in practice. For example, a self-consistent calculation for two oxygen vacancies 4.98 Å apart produces two impurity states around 0.7 below the conduction band, separated in energy by about 0.04 eV.

The charge distribution in clusters of vacancies suggests a model for samples with multiple vacancies in which the screening charge at a given site is given by adding the screening charges due to neighboring vacancies, treated as independent. We present some examples of the results of such a model below.

VI. COMPARISON WITH EXPERIMENTS

At this point it is interesting to compare our calculation with optical and other experiments. Since the first infrared-absorption experiments[6] on reduced rutile, it has generally been assumed that oxygen vacancies are responsible for the impurity band 0.7 eV below the conduction-band edge, despite evidence from various diffusion experiments[7] showing the importance of titanium interstitials. In the model used here, titanium interstitials at low concentrations produce a band of states leading to an absorption peak very close in position to the experimental absorption peak. Our calculated impurity band at these low impurity densities is, however, much narrower than the experimentally observed one.

In the case of oxygen vacancies, our model will result in an absorption peak at 0.7 eV. Our model for the vacancy, however, has one more empirical parameter (the constant in the diagonal matrix element for the s orbital on the vacancy site) than the model for the interstitial does. This parameter was adjusted to give an absorption peak at the experimentally observed value, so the coincidence of the calculated and observed peaks is due to fitting and does not constitute evidence either for the validity of the model or in favor of oxygen vacancies as the dominant point defect. As in the case of interstitials, we predict a narrower impurity band than the observed one. For pairs of vacancies, we predict two states, one at about 1.1 eV and the other around 0.35 eV below the conduction-band edge.

The oxygen deficiency of the samples studied in Ref. 6 is reported to be 10^{-3}. This means that one of every 10^3 oxygen atoms is missing in the crystal. If the defects were completely randomly distributed without correlation in the crystal, then the concentration of pairs and higher-order clusters would be completely negligible, and broadening effects due to such clusters could not account for the width observed. We suggest two possible origins for the width: (1) Charge fluctuations may result in fluctuations in the local self-consistent potential (the diagonal matrix elements in our calculations) leading to a distribution of energies of the local donor levels; and/or (2) the distribution of defects may not be random, leading to more clusters than the assumption of uncorrelated randomness in the distribution would predict. We discuss these possibilities in turn.

With regard to the first possibility, we illustrate the effect with a calculation on a larger sample ($8\times8\times8$ unit cells or 3072 atomic sites), in which we make the approximation suggested in Sec. IV: We assume that the screening charges due to multiple defects are, at each site, just the sum of the screening charges due to each defect alone in the crystal. We showed in Sec. IV that this approximation worked quite well for pairs of vacancies, but its validity for hundreds of vacancies (as in this application) has not been determined, and we expect that it will exaggerate the extent of charge fluctuation. We make the calculation of the total density of states in this case using the equation of motion techniques described in Ref. 11. This method is restricted to quite large defect concentrations, and we show the results for 0.5%, 1%, and 5% of oxygen vacancies in Fig. 6. We see that the charge fluctuation effect results in very significant broadening of the levels, even at 1% concentrations. It appears, however, that this is not sufficient to account for the observed width, since the calculation for 0.5% vacancies gives a smaller impurity bandwidth than that measured in the experiments. Furthermore, this approximation may exaggerate the width of the impurity band, because it fails to take account of possible screening of large length scale charge fluctuations.

The second possible contributing origin of the observed width is correlations in the spatial defect distribution. It is known[19–21] that the stable phases of reduced rutile are Magneli phases which may be regarded as consisting of ordered arrays of planar defects. We think it likely that reduced samples such as those used in the infrared-absorption experiments of Ref. 6 may be partly phase separated into regions of stoichiometric rutile and partially formed planar defects which may be regarded as clusters of interstitials and vacancies. This possibility has been extensively discussed by others[22–24] in the context of the interpretation of structural and diffusion measurements, and by use of empirical modeling of interatomic forces. In such a model, significant broadening of the infrared peak might result, arising from the electronic donor levels associated with these various defect clusters.

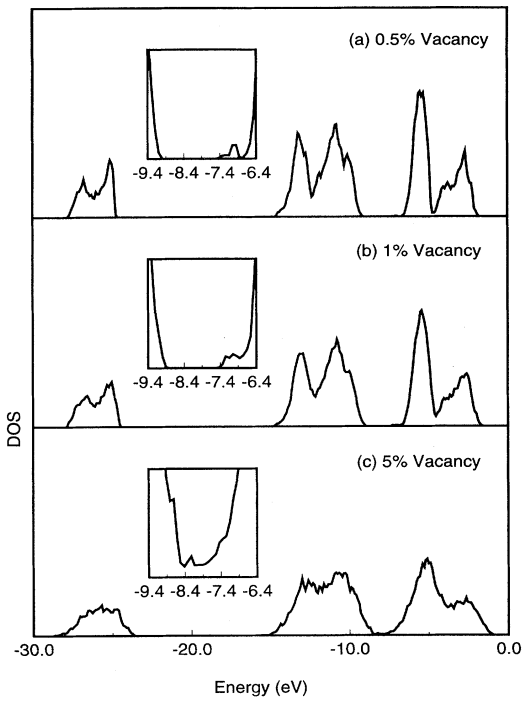

FIG. 6. Density of states of a cluster of (8×8×8) rutile unit cells, with various concentrations of oxygen vacancy randomly distributed. At 0.5% oxygen vacancy, the impurity band is sharply peaked around −7 eV, 0.7 eV below the conduction-band edge. At higher concentrations of vacancy, the impurity band broadens. The insets in the graphs show the density of states around the band gap of rutile.

To model such a structure, one would need to include correlations in the distribution of point defects, thus increasing the number of clusters, relative to the number expected in an uncorrelated random distribution. We have explored the energetics of interstitial clustering, without considering the ionic relaxation around the interstitials, and without considering the ion-ion interaction beyond the simple Coulombic interaction. We found that in our model the interactions between the interstitials are repulsive. For example, one pair of interstitials 4.59 Å apart has an energy 0.36 eV higher than the energy of a pair 9.18 Å apart.

VII. DISCUSSION AND CONCLUSIONS

Our self-consistent models for the titanium interstitial and the oxygen vacancy show that these defects are screened over very short (but not zero) distances, as we previously assumed in a one-electron model.[11] Our calculation of the structure of the titanium interstitial predicts a level at 0.8 eV below the conduction-band edge without any parameter adjustment, suggesting that the titanium interstitial could account for the position of the observed[6] infrared-absorption band, which is usually ascribed to oxygen vacancies. On the other hand, we find that point defects interact very weakly at large distances, making it difficult to account for the observed width of the infrared band, if the point defects are distributed at random and without correlation in the crystal. We suggest that the defects may not be distributed in this random, uncorrelated manner in the real crystal, but that instead they cluster as a consequence of partial phase separation into stoichiometric rutile and incipient crystalites of Magneli phase. Such structures have previously been studied using empirical modeling of interatomic forces,[22] but without regard for the electronic structure of the resulting defects. From the point of view of those atomic force models, we note that our results show that the charges assumed for titanium interstitials in those models (+3 or +4) are almost certainly too high by a significant factor, since atomic relaxation (which we have not yet included in our calculations) is unlikely to increase the value of the interstitial charge (+1.58) which we find.

We also find that, at least for oxygen vacancies, a model for multiple defects in which the screening charges due to each defect individually are simply added at each site is likely to be quite accurate. We can use such a model to indicate the effects of multiple defects with results shown in Fig. 6. In particular, one sees that for defect concentrations of 1% or less (as one certainly has in the experiments of Ref. 6), the impurity band remains extremely narrow, inconsistent with experiment. This suggest that, as noted above, defect clustering is likely to be occurring. To take quantitative account of such effects, we require a model in which both electronic structure and atomic relaxation are taken into account in these systems. This will be the subject of future work.

ACKNOWLEDGMENTS

This work is supported by the DOE under Grant No. DE-FG02-91-ER45455 and the Minnesota Supercomputer Institute. The following people contributed to the development of some of the computer codes used in this work: M. Michalewicz, H. Shore, and N. Tit. H. Shore also contributed to the formal development of our approach.

APPENDIX: FORMAL DESCRIPTION OF THE METHOD

We start[25] with the general variational principle with respect to the density $n(\mathbf{r})$:

$$\delta E(\{n(\mathbf{r}\})/\delta n(\mathbf{r})=0 , \tag{A1}$$

where $E(\{n(\mathbf{r}\})$ is the expectation value of the energy in the ground state. The energy contains three terms: kinetic energy T, a one-electron potential energy V_1, and the electron-electron Coulomb interaction energy V_2. These are expressed as

$$T=\int d\mathbf{r} \lim_{\mathbf{r}\to\mathbf{r}} \frac{\hbar^2}{2m}\nabla_{\mathbf{r}}\cdot\nabla_{\mathbf{r}'}\rho_1(\mathbf{r};\mathbf{r}') , \tag{A2}$$

$$V_1=\int d\mathbf{r}\,\rho_1(\mathbf{r};\mathbf{r})v_1(\mathbf{r}) , \tag{A3}$$

$$V_2=(\tfrac{1}{2})\int d\mathbf{r}d\mathbf{r}'\rho_2(\mathbf{r},\mathbf{r}';\mathbf{r},\mathbf{r}')\frac{e^2}{|\mathbf{r}-\mathbf{r}'|} . \tag{A4}$$

Here $\rho_1(\mathbf{r};\mathbf{r}')$ and $\rho_2(\mathbf{r},\mathbf{r}';\mathbf{r},\mathbf{r}')$ are one- and two-body density matrixes defined as

$$\rho_1(\mathbf{r};\mathbf{r}') \equiv \int d\mathbf{r}_2 \ldots \times \int d\mathbf{r}_N \Phi_N^*(\mathbf{r},\mathbf{r}_2,\ldots,\mathbf{r}_N) \times \Phi_N(\mathbf{r}',\mathbf{r}_2,\ldots,\mathbf{r}_N) , \tag{A5}$$

$$\rho_2(\mathbf{r},\mathbf{r}';\mathbf{r},\mathbf{r}') \equiv \int d\mathbf{r}_3 \ldots \times \int d\mathbf{r}_N \Phi_N^*(\mathbf{r},\mathbf{r}',\mathbf{r}_3,\ldots,\mathbf{r}_N) \times \Phi_N(\mathbf{r}',\mathbf{r},\mathbf{r}_3,\ldots,\mathbf{r}_N) , \tag{A6}$$

in which $\Phi_N(r_1,\ldots,r_N)$ is the ground-state wave function. (In these expressions, the integrals are meant to include sums over the discrete spin variable.)

We express the energy in terms of eigenfunctions $\psi_\lambda(\mathbf{r})$ of the one-particle density matrix, expressed as an integral operator:

$$\int \rho_1(\mathbf{r},\mathbf{r}')\psi_\lambda(\mathbf{r}')d\mathbf{r}' = n_\lambda \psi_\lambda(\mathbf{r}') , \tag{A7}$$

It is not hard to show[14] in general that $0 \le n_\lambda \le 1$. Here we assume, as in Hartree-Fock and local-density approximation (LDA) approximations, that the n_λ's are equal to either 1 or to 0, and are interpreted as occupation numbers of one-electron orbitals. We use a tight-binding basis and expand $\psi_\lambda(\mathbf{r})$ as

$$\psi_\lambda(\mathbf{r}) = \sum_{i,\nu} \phi_{i,\nu}(\mathbf{r}) \langle i\nu|\lambda\rangle , \tag{A8}$$

where $\phi_{i,\nu}(\mathbf{r})$ is orbital ν localized at site i. The $\phi_{i,\nu}(\mathbf{r})$'s are orthonormal. The terms T and V_1 then become

$$T + V_1 = \sum_{i,\nu;j,\nu'} Q_{i,\nu;j,\nu'}(t_{i,\nu;j,\nu'} + v^{(1)}_{i,\nu;j,\nu'}) , \tag{A9}$$

in which

$$Q_{i,\nu;j,\nu'} = \sum_\lambda n_\lambda \langle i,\nu|\lambda\rangle\langle\lambda|j,\nu'\rangle \tag{A10}$$

and

$$t_{i,\nu;j,\nu'} = \int d\mathbf{r}\, \phi^*_{i,\nu}(\mathbf{r}) \left[\frac{-\hbar^2\nabla^2}{2m}\right] \phi_{j,\nu'}(\mathbf{r}) , \tag{A11}$$

$$v^{(1)}_{i,\nu;j,\nu'} = \int d\mathbf{r}\, \phi^*_{i,\nu}(\mathbf{r}) v_1(\mathbf{r}) \phi_{j,\nu'}(\mathbf{r}) . \tag{A12}$$

The sum

$$Q_i \equiv \sum_\nu Q_{i,\nu;i,\nu} \tag{A13}$$

can be interpreted as the number of electrons at site i.

We introduce approximations for the calculation of term V_2 by separating intersite from intrasite terms in the expansion of ρ_2 in the tight-binding basis. For intersite terms, we assume that the Hartree-Fock approximation is adequate, while we assume that intrasite terms contribute an energy of the form $\sum_i E_i(Q_i)$ depending only on the total number of electrons on the site. We determine $E_i(Q_i)$ from experimental ionization potentials. The energy then becomes

$$E = \sum_i E_i(Q_i) + \sum_{i\neq j,\nu,\nu'} Q_{i,\nu;j,\nu'}(t_{i,\nu;j,\nu'} + v^{(1)}_{i,\nu;j,\nu'}) + \tfrac{1}{2}\sum_{i\neq j} \frac{e^2 Q_i Q_j}{\mathbf{R}_{ij}} - \tfrac{1}{2}\sum_{i\neq j,\nu,\nu'} \delta_{\sigma_\nu\sigma_{\nu'}} \frac{e^2 Q^2_{j,\nu';i,\nu}}{R_{ij}} , \tag{A14}$$

assuming in the Hartree and exchange integrals that overlaps between the localized orbitals on different sites can be neglected and that the integrals

$$\int\int d\mathbf{r}\cdot d\mathbf{r}' \frac{|\phi_{i,\nu}|^2 |\phi_{j,\nu'}|^2}{|\mathbf{r}-\mathbf{r}'|} \tag{A15}$$

may be approximated as

$$\frac{1}{|\mathbf{R}_i - \mathbf{R}_j|} \equiv 1/R_{ij} , \tag{A16}$$

where $\mathbf{R}_i$ and $\mathbf{R}_j$ are the positions of sites i and j, respectively.

The effective one-electron equation is obtained by varying $\psi_\lambda = \sum_{i,\nu}\phi_{i,\nu}(\mathbf{r})\langle i,\nu|\lambda\rangle$ through variation of the coefficients $\langle i,\nu|\lambda\rangle$, assuring normalization in the usual way through addition of a term $-\sum_\lambda \epsilon_\lambda \int |\psi_\lambda(\mathbf{r})|^2$ to the energy functional and maintaining the constraint that n_λ be equal to the number of electrons by use of the chemical potential (Fermi energy) μ_c as a Lagrangian multiplier. The result is Eq. (1).

[1] V. E. Henrich, Rep. Prog. Phys. **48**, 1481 (1985).
[2] K. M. Glassford and J. R. Chelikowsky, Phys. Rev. B **46**, 1284 (1992).
[3] K. Vos, J. Phys. C **10**, 917 (1977).
[4] B. Poumellec, P. J. Durham, and G. Y. Guo, J. Phys. Condens. Matter **3**, 8195 (1991).
[5] N. Casillas, S. R. Snyder, W. H. Smyrl, and H. S. White, J. Phys. Chem. **95**, 7002 (1991).
[6] D. C. Cronemeyer, Phys. Rev. **113**, 1222 (1959).
[7] A. Atkinson, in *Advances in Ceramics,* edited by C. R. A. Catlow and W. C. Mackrodt (The American Chemical Society, Westerville, OH, 1987), Vol. 23, p.3.
[8] X. Hoshino, N. L. Peterson, and C. L. Wiley, J. Phys. Chem. Solids **46**, 1397 (1985).
[9] S. Munnix and M. Schmeits, Phys. Rev. B **31**, 3369 (1985).
[10] J. W. Halley and H. B. Shore, Phys. Rev. B **36**, 6640 (1987).

[11]J. W. Halley, M. T. Michalewicz, and N. Tit, Phys. Rev. B **41**, 10 165 (1990).
[12]N. Tit, J. W. Halley, and M. T. Michalewicz, Surf. Interf. Anal. **18**, 87 (1992).
[13]M. Ramamoorthy, R. D. King-Smith, and D. Vanderbilt, Phys. Rev. B **49**, 7709 (1994).
[14]N. Yu and J. W. Halley (unpublished); Mater. Sci. Forum (to be published).
[15]D. M. Heyes, M. Barber, and J. H. R. Clarke, J. Chem. Soc. Fardaday Trans. **2:73**, 1485 (1977).
[16]T. Koopmans, Physica **1**, 104 (1933).
[17]B. Silvi, N. Fourati, R. Nada, and R. A. Catlow, J. Phys. Chem. Solids **52**, 1005 (1991).
[18]M. Aono and R. R. Hasiguti, Phys. Rev. B **48**, 12 406 (1993).
[19]S. Anderson and A. Magneli, Naturwissenschaften **42**, 495 (1956).
[20]L. A. Bursill and B. G. Hyde, Prog. Solid State Chem. **7**, 177 (1972).
[21]R. F. Bartholomew and D. R. Frenkl, Phys. Rev. **187**, 828 (1969).
[22]A. N. Cormack, C. M. Freeman, C. R. A. Catlow, and R. L. Royle, *Advances in Ceramics* (Ref. 7), p. 283.
[23]M. G. Blanchin, L. A. Bursill, and D. J. Smith, Proc. R. Soc. London Ser. A **391**, 351 (1984).
[24]L. A. Bursill, G. J. Shen, D. J. Smith, and M. G. Balanchin, Ultramicroscopy **13**, 191 (1984).
[25]P. Hohenberg and W. Kohn, Phys. Rev. **136**, B864 (1964).